Supplementary Materials for

Cortical Information Flow During Flexible Sensorimotor Decisions

Markus Siegel, Timothy J. Buschman, and Earl K. Miller

This PDF file includes

Materials and Methods

Subjects and recordings

Experiments were performed in two rhesus monkeys (one male, one female). All procedures followed the guidelines of the Massachusetts Institute of Technology Committee on Animal Care and the National Institutes of Health. Each monkey was implanted with a titanium head bolt to immobilize the head. Following the behavioral training, three titanium recording chambers were stereotactically implanted over frontal, parietal, and occipitotemporal cortices in the left hemisphere. Through these chambers, we simultaneously implanted Epoxy-coated tungsten electrodes in the lateral prefrontal cortex, frontal eye fields, lateral intraparietal cortex, inferotemporal cortex (TEO), visual area V4, and the middle temporal area (MT). Electrodes were lowered using custom-built microdrive assemblies that lowered electrodes in pairs or triplets from a single screw. These microdrive assemblies were designed for a high density of electrodes (1 mm spacing for pairs or 0.7 mm triangular spacing for triples) to maximize the number of simultaneously recorded neural signals across the six regions of interest. The electrodes were acutely lowered through the intact dura at the beginning of every recording session. Electrodes were simultaneously advanced in pairs or triplets of electrodes with penetrations typically angled relative to the cortical surface. We did not aim for a specific layer or fine-tune the positioning for specific cells. Thus, recordings were from all cortical layers with no bias for a specific depth. Electrodes were allowed to settle for a minimum of 1 h before recording. After each recording session, electrodes were retracted and the microdrive assemblies were removed from the recording chambers.

Neuronal activity was recorded across a maximum of 108 electrodes simultaneously. All signals were referenced to ground and recorded broad-band at 40 kHz. Offline, we extracted the continuous time-course of multi-unit spiking activity (MUA by filtering the broad-band signal between 500 Hz and 6 kHz (2^{nd}-order zero-phase forward-reverse Butterworth filter), rectification, low-pass filtering at 250 Hz (2^{nd}-order zero-phase forward-reverse Butterworth filter), and resampling at 1 kHz (*29*, *30*).

Behavioral Task

Monkeys were trained on a flexible visuomotor decision making task. All stimuli were displayed on a color calibrated CRT monitor at 100 Hz vertical refresh rate. An infrared-based eye-tracking system continuously monitored eye position at 240 Hz. Behavioral control of the behavioral task was handled by the Monkeylogic program (www.monkeylogic.net) (*31*, *32*).

Each trial was initiated when the animal fixated on a point at the center of the screen. Fixation was required within 1.2° of visual angle of the fixation point. After a short fixation period (500 ms), the animal was presented with a visual task cue for 1000 ms. Cues were four different gray shapes (Fig. 1C) of about 1.5° visual angle diameter that were presented centrally on the fixation spot. Two of the four shapes cued the motion and color task, respectively (Fig. 1C). Using two cues for each task allowed us to dissociate neuronal information about the cue (the visual shape of the cue) and neuronal information about the task at hand (motion vs. color).

After the cue period, the cue was switched off and a stimulus was presented centrally on the fixation spot. Stimuli were colored dynamic random dot patterns with 100% motion coherence presented centrally on the fixation spot (stimulus diameter : 3.2°; dot diameter: 0.08°; number of dots: 400; dot speed: 1.67°/s or 10°/s for half of the recording sessions, respectively). To prevent learning of dot patterns, new stimuli were generated for each recording session. To rule out effects of stimulus variability on neuronal choice information, the same stimulus (dot pattern) was used for all trials per recording session. On each trial, all dots moved in the same direction and had the same color. There were 7 possible stimulus colors and 7 possible motion directions. Colors and motion directions were chosen to optimize perceptual equidistance and equivalence within and between feature dimensions (Fig. S1). 4 motion directions spanned the range between upward (90º) and downward (-90º) motion through rightward motion (0º) in 60º steps (-90º, -30º, 30º, 90º). In addition, 3 motion directions were placed on (0º) and near (-5º, 5º) the category boundary (right). Similarly, 4 colors spanned the range between red (90º) and green (-90º) through yellow (0º) in 60º steps (-90º, -30º, 30º, 90º). In addition, 3 colors were placed on (0º) and near (-5º, 5º) the category boundary (yellow). To optimize perceptual homogeneity, all colors were defined in the CIE L*a*b* space and had the same luminance and saturation.

Depending on the task cued at the beginning of each trial, the animals categorized either the color (red vs. green) or motion direction (up vs. down) of the stimulus and reported their percept with a left or right saccade. The stimulus-response mapping for each task was fixed (Fig. 1C). Two saccade targets were displayed 6º to the left and right of the fixation spot throughout the trial. Animals had to respond with one direct saccade to one of these targets. Animals were free to respond at any time up to 1s after stimulus onset (Fig. 1A). For correct responses, animals were rewarded with apple juice. Animals were always rewarded for ambiguous trials with stimuli on the category boundary (yellow and right for color and motion task, respectively). These ambiguous trials were excluded for calculating the animals' percent correct performance.

Recording locations

We recorded multi-unit spiking activity (MUA) from a total of 2694 recording sites (1753 and 941 for the two monkeys) in 48 recording sessions (31 and 17 for the two monkeys) across all six investigated regions: FEF: 532 sites, dlPFC: 1020 sites, LIP: 807 sites, IT: 57 sites, V4: 155 sites, MT: 123 sites. We recorded from up to 108 electrodes simultaneously per session (mean/STD: 56/17 electrodes). For each session, we recorded at least from three regions simultaneously. Across all sessions, all pairs of regions were at least once recorded simultaneously.

Recordings were performed through three recording chambers that were stereotactically placed over frontal (FEF and PFC recordings), parietal (LIP recordings), and occipitotemporal (MT, V4 and IT recordings) cortex according to detailed 3D planning using custom MATLAB software and based on high-resolution structural MRIs of each animal. Frontal, parietal and occipitotemporal recording chambers were placed about 28 mm anterior, 2 mm posterior, and 1 mm posterior to the interaural plane, respectively.

The area definition of each recording site was based on the stereotactic recording location, on neuronal responses in a functional mapping task, and on microstimulation results. To this end, before recording the main task, we functionally characterized recording locations in several recording sessions during passive fixation with manually controlled visual stimuli and automatically flashed colored dynamic random dot patterns. Furthermore, on each recording session and in addition to the main task, the animals performed a functional mapping task. During central fixation, brief (150 ms) dynamic random dot patterns of different motion directions and colors were passively flashed on the fixation spot. Stimulus parameters were identical to the stimuli used during the main task. Motion directions and colors spanned the entire direction and hue space with 30º spacing. These stimuli were used to characterize the visual responsiveness and tuning of the recorded spiking activity. Following the flashed stimuli and a brief delay, a brief (100 ms) spot of light was flashed at one out of six different locations in the periphery. After a memory delay (750 ms), the fixation point was extinguished and the animal made a saccade to the remembered location of the light spot. This delayed saccade task was used to isolate LIP from surrounding regions, as it is the only region in the parietal cortex that shows spatially selective memory delay activity (*33*). Recording sites in the lateral bank of the intraparietal sulcus with significant spatially selective memory delay activity ($p < 0.05$) and/or significant ($p < 0.05$) visual responses to the random dot patterns in the functional mapping task were classified as LIP.

We used microstimulation to demarcate FEF from dlPFC in the frontal recording chamber. An isolated pulse stimulator was used for electrical stimulation. Stimulation was delivered as a 200 ms train of biphasic pulses with a width 400 μs and an pulse frequency of 330 Hz. Stimulation was performed using the same electrodes as for recording. Stimulation current

was started at 150 μA and reduced to find the threshold at which an eye movement vector was elicited 50% of the time. Sites that had thresholds of stimulation amplitudes <50 μA were classified as FEF (*34*). Anterior sites were classified as lPFC.

Occipitotemporal recording sites were classified as MT, V4 and TEO based on their anatomical location and if they showed significant ($p < 0.05$) visual responses to the random dot patterns in the functional mapping task. MT recordings sites were in the lower and medial bank of the posterior third of the superior temporal sulcus. V4 recording sites were posterior and ventral to MT sites on the angular gyrus. TEO recording sites were on the lateral convexity of the inferior temporal gyrus between the ascending part of the inferior occipital sulcus and the posterior middle temporal sulcus.

Information encoded by neuronal spiking activity

We quantified the information encoded by multi-unit spiking activity (MUA) about several task factors. Specifically, we used an analysis of variance (ANOVA) to quantify the percentage of MUA variance across trials that could be explained by the following task factors: the identity of the cue presented at the beginning of each trial, the task (motion vs. color categorization) to be performed, the motion direction of the categorized stimulus, the color of the categorized stimulus, and the animals' motor choice (left vs. right saccade).

To quantify these types of information we computed a 7-way ANOVA across trials. The first three factors of the ANOVA corresponded to the cue of each trial grouped into two levels according to all three possible pairwise pairings of the four task cues. The first factor corresponded to the cue pairing that reflected the assignment of the cues to the tasks (cross or flower (motion) vs. circle or triangle (color); Fig. 1C). The second and third factors corresponded to the two other cue pairings that did not reflect the cue-task assignment (cross or circle vs. flower or triangle; cross or triangle vs. flower or circle). This construction of these three factors ensured equal statistical properties between factors (balanced number of trials and levels) and fully capturing cue as well as task related spiking variance. Spiking activity that was selective for any or multiple of the four cues yielded non-zero explained variance for any of the three factors. In contrast, spiking activity that was selective for the task (motion vs. color) irrespective of the specific cue yielded non-zero explained variance only for the first of the three factors. Thus, we computed cue information as the average explained variance of all first three factors, and task information as the variance explained by the first factor minus the average variance explained by the second and third factor. The fourth and fifth factor of the ANOVA were the motion direction (7 levels) and color (7 levels) of the stimulus on each trial, respectively. The sixth factor was the choice of the animal on each trial (2 levels, left vs. right). The seventh factor was the choice of the animal on the previous trial (2 levels, left vs. right). Including the choice on the previous trials as a task factor allowed us to quantify choice-predictive

information independent from any potential choice-sequence effects. In other words, we could quantify neuronal information predicting the upcoming choice independent of the last choice.

We quantified neuronal information about each task factor independently. Importantly, the investigated task factors were not orthogonal. E.g., for the motion and color task, motion direction and color were highly correlated with choice, respectively (motion task: $r^2_{\text{motion x choice}} = 0.5$, $r^2_{\text{color x choice}} = 0.002$; color task: $r^2_{\text{motion x choice}} = 0.005$, $r^2_{\text{color x choice}} = 0.5$; all $P < 10^{-16}$ Spearman rank correlation). Thus, we computed an unbalanced ANOVA, that implicitly orthogonalized the different task factors. In other words, we quantified the spiking variance explained be each factor that could not be explained by any of the other factors. E.g., as choice information we measured only the information about the monkeys' choice that was not explained by cue, task, color, motion or the previous choice.

We quantified cue and task information across both tasks. We quantified motion, color and choice information separately for each task (motion vs. color categorization). We then pooled motion, color, and choice information across tasks for several analyses (Figs. 1F, 1H, 2, 3, and 4). If motion and color information is computed across all trials per task, the amount of motion and color information has a different scaling for the motion and color tasks, because both factors have a different correlation with the factor choice depending on the tasks (see correlation statistics above). There is less motion and color information for the corresponding tasks respectively, because there is stronger correlation of these factors with the choice. To rule out this effect for the quantitative comparison of motion and color information between tasks (Fig. 1I), we computed the ANOVA analysis separately for trials from the four quadrants of the stimulus space (Fig. 1B) and both choices. Thus, choices are held constant for each group of trials. We then averaged motion and color information across quadrants and correct choices. To quantify the amount of significantly encoding units (Fig. 1G) we tested for a significant encoding across all trials and both tasks for all types of information.

We estimated the amount of variance explained by each factor ω^2 as

$$\omega^2 = \frac{SS_{Between\ Groups} - df * MSE}{SS_{Total} + MSE}$$

, where $SS_{Between\ Groups} = \sum_{group}^{G} n_{group} * (\bar{x}_{group} - \bar{x})^2$ is the sum of squares between G groups (i.e., levels), $SS_{Total} = \sum_{i}^{N} (x_i - \bar{x})^2$ is the total sum of squares across N trials, $df = G - 1$ are the degrees of freedom, and $MSE = \sum_{i}^{N} (x_i - \bar{x}_{group})^2$ is the mean squared error. ω^2 is an unbiased estimator of explained variance (*35*). In particular, and in contrast to the estimator η^2, ω^2 yields a zero-mean statistic under the Null-hypothesis of no explained variance independent of small sample size N. For each factor of the ANOVA, i.e. for each type of information, we assessed the statistical significance of explained variance

ω^2 using a non-parametric permutation statistic. We compared the measured explained variance to an empirical null-distribution generated by randomly permuting the trial-condition assignment (1000 permutations).

To estimate the time-course of neuronal information, we performed a sliding-window ANOVA shifting a 50 ms window across the trial in 5 ms steps. For all latency estimates, the resulting information time-courses were smoothed with a 50 ms (full width at half maximum) Hanning window. To investigate information dynamics relative to cue and stimulus onset, trials were temporally aligned to stimulus onset (Figs. 2 and 3). To rule out confounds of neuronal information due to the motor response itself in this stimulus-locked analysis, for each trial, we only included neuronal activity up to 5 ms before saccade onset.

To investigate the build-up of choice predictive information before the animals' response, trials were temporally aligned to the choice (saccade onset) (Fig. 4). An important, but typically neglected, caveat for such response-locked analysis is that a difference in average response time between choices can induce spuriously measured choice information. This is because, for different response times between choices, stimulus-locked changes in neuronal activity (e.g., phasic responses to stimulus onset) do not temporally align between choices relative before the response. This temporal misalignment of stimulus-locked changes then leads to erroneously quantifying a difference in neuronal activity as predicting the upcoming choice. To rule out that this confounded choice information, for the response-locked analysis, we equated reaction times between choices by stratification. For each stimulus condition (motion direction, color, and task), we randomly removed trials for both choices to match the response time distributions for both choices. Before stratification, both animals had significantly different reaction times between choices for many stimulus conditions ($p < 0.05$, for 31 and 32 out of 42 motion x color x task conditions). After stratification, no significant differences remained ($p > 0.05$, for both animals and all motion x color x task conditions).

To quantify average amounts of information per region we averaged information time courses across the following time windows (Fig. 1 H and I). Cue and task information: 0.5 s – 1 s post cue (second half of the cue interval); motion and color information: 1.0 s – 1.27 s post cue (stimulus onset to average response latency); choice information: 0.2 s – 0 s pre response (200 ms before response) and -0.5 s – 1 s post cue (pre-stimulus interval).

Information dynamics

We estimated the latency of information as the time at which information reached half its maximum. In contrast to measures based on the time at which information reaches statistical significance, the employed measure is robust to differences in the strength of information or the amount of data. Latencies were not estimated if there was no significant

information ($P > 0.05$) in the interval of interest. This was the case for the transient peak of task information being absent in MT, LIP, PFC and FEF. Furthermore, latencies were not estimated if there was no significant increase (linear regression, $P > 0.05$) of information in the interval of interest. This was the case for pre-response choice information in IT.

Choice information was already significant before stimulus onset in most regions. We ruled out that differences in such pre-stimulus choice information between regions lead to spurious latency differences. To this end, for each region, we subtracted the baseline choice information before estimating half maximum latencies (Fig. 4).

For statistical comparisons of latencies between regions and types of information we estimated the standard error of latencies by bootstrap across units (100 resamples). We then assessed the significance of latency differences using *T*-statistics.

All analysis code was custom written in Matlab and C.

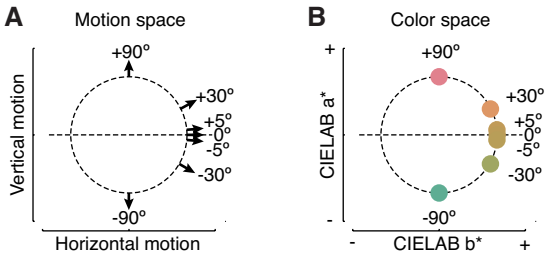

Fig. S1. Stimulus space. Stimuli covered motion direction and color spaces between opposite motion directions (up/down through right) and colors (red/green through yellow). All stimuli were 100% coherent, iso-luminant, and iso-saturated. The circular display illustrates the analogy between both stimulus features. (**A**) Employed motion directions. (**B**) Employed colors. Horizontal dashed lines represent the categorization boundaries.

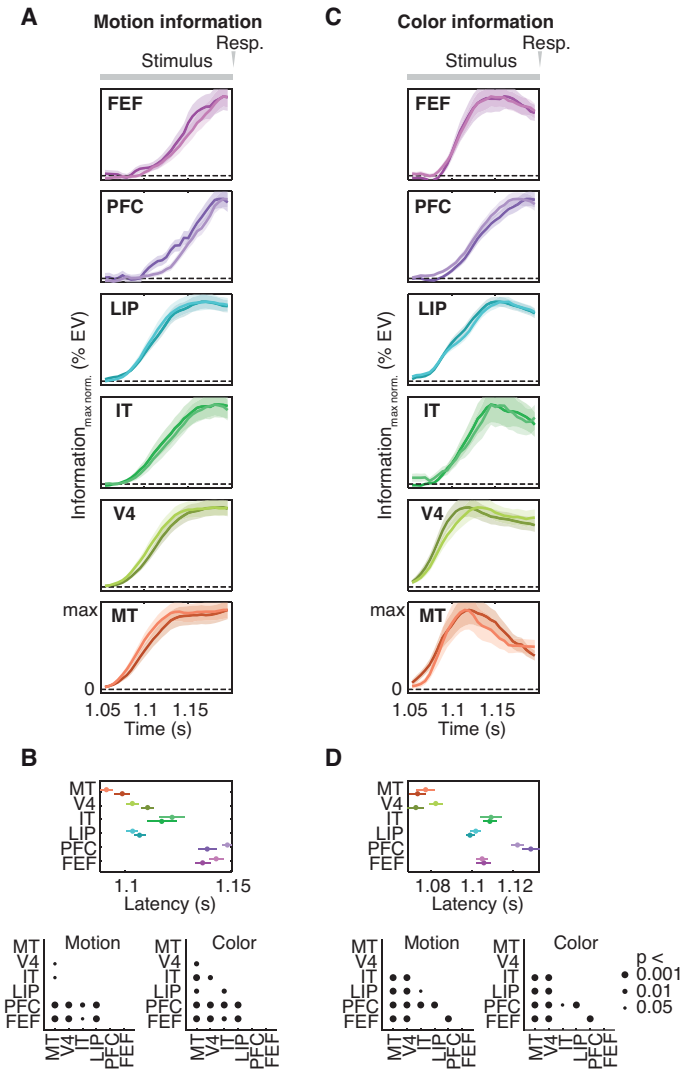

Fig. S2. Dynamics of motion and color information during motion and color categorization tasks. (**A**) Time-courses of neuronal information about motion direction of the categorized stimulus. Panels display time-courses of information normalized by maximum information. (**B**) Comparison of motion information latencies between regions (half maximum information). Black dots in the bottom panels indicate significant latency differences between regions. (**C**) Time-courses of information about the color of the categorized stimulus across regions. Same conventions as in (A). (**D**) Comparison of color information latencies between regions. Same conventions as in (B). All error bars denote SEM. Dark and bright colors correspond to motion and color tasks, respectively.

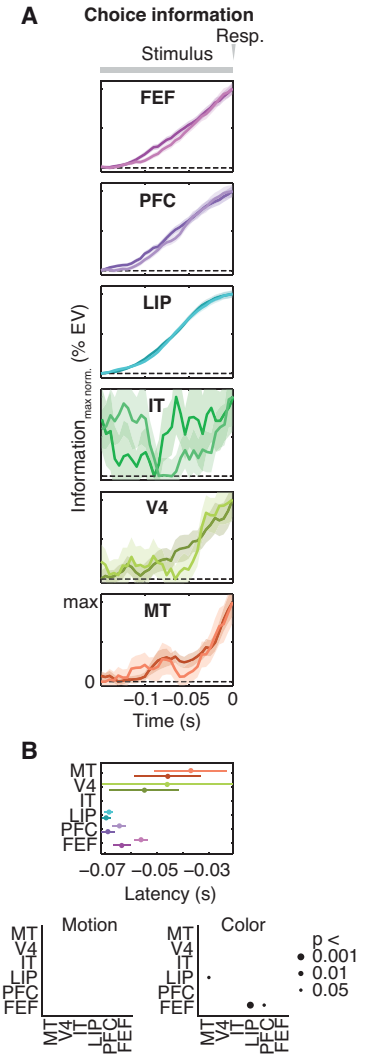

Fig. S3. Dynamics of choice information for motion and color categorization tasks. (**A**) Response locked time-courses of neuronal information about the animas' choice. Panels display information time-courses normalized by maximum information. (**B**) Comparison of stimulus-locked choice information latencies between regions (half maximum information). Black dots in the bottom panels indicate significant latency differences between regions. Latencies were not estimated for IT because there was no significant increase of information in IT in the investigated interval (linear regression, $P > 0.05$). All error bars denote SEM. Dark and bright colors correspond to motion and color task, respectively. There were no significant latency differences for the motion task.

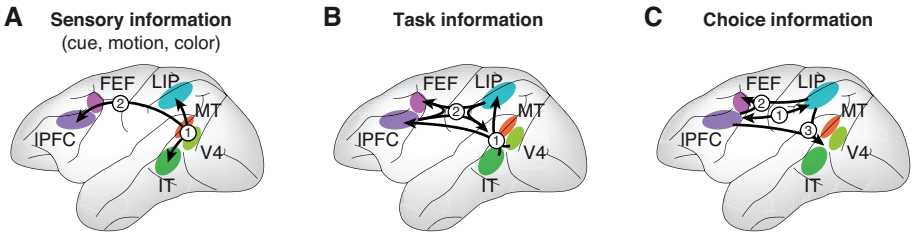

Fig. S4. Schematic information flow during sensorimotor decisions. (**A**) All three types of sensory information (cue, motion, and color) flowed bottom-up from MT and V4, to LIP, IT, FEF and PFC. (**B**) Task information was first extracted in a transient burst in V4 and IT, from where it fed forward to PFC and LIP. Then there was a top-down flow of sustained task information from PFC and LIP to FEF and visual cortex. (**C**) Choice signals simultaneously built up in PFC and LIP. Then choice signals flowed to FEF and visual cortex.